

# Inhibition of Switch-on Fluorescence of Fluorochrome on Loading TiO<sub>2</sub> with Gold

**Dhanalekshmi K.I**

Beijing Institute of Technology

**Chengchen Jiang**

South China University of Technology

**Jayamoorthy K** (✉ [kjmche@gmail.com](mailto:kjmche@gmail.com))

St. Joseph's College of Engineering

**Magesan P**

Bharath University

**Oguejiofo T. Ujam**

University of Nigeria, Nsukka

**Xiang Zhang**

Beijing Institute of Technology

---

## Research Article

**Keywords:** Fluorochrome, Gold loaded TiO<sub>2</sub> nanoparticles, Fluorescence, Electron transfer

**Posted Date:** January 8th, 2021

**DOI:** <https://doi.org/10.21203/rs.3.rs-140474/v1>

**License:**   This work is licensed under a Creative Commons Attribution 4.0 International License.

[Read Full License](#)

---

# Abstract

Gold loaded TiO<sub>2</sub> nanoparticles have been synthesized and characterized by powder XRD, HR-TEM, and EDX analysis. The binding interaction of fluorescent sensor 5-amino-2-mercaptobenzimidazole (fluorochrome) with TiO<sub>2</sub> and gold loaded TiO<sub>2</sub> nanoparticles has been discussed herein. The interaction of fluorochrome with TiO<sub>2</sub> and gold loaded TiO<sub>2</sub> nanoparticles has been studied by UV-visible, fluorescence, and FT-IR spectral techniques. The fluorescence emission occurs at 421 nm and this has been selectively enhanced by TiO<sub>2</sub> nano semiconductor. This technique is sensitive to detect and estimate TiO<sub>2</sub> nano semiconductor at a micromolar level. This switch-on fluorescence is suppressed when it is loaded with gold. The strong adsorption of fluorochrome over the surface of nano semiconductor results in the electron transfer between fluorochrome and nano semiconductor. Further, the binding site of nano semiconductor with fluorochrome has been studied theoretically by using the molecular electrostatic potential (MEP). The results show higher electron density at the azomethine nitrogen atom.

## 1. Introduction

Among families of heterocyclic compounds, imidazoles play an important role because of its bioactivity and sensor properties. Imidazole and its derivatives have attracted increasing interest in the field of chemical research because it acts as a precursor in synthetic reactions towards, primarily for the preparation of functionalized materials. Some of the well-known bio-components of human organisms such as Vitamin B<sub>12</sub>, amino acid histidine, DNA base structure components, histamine, purines, and biotin contain the imidazole nucleus as the main structure. Several synthetic drug molecules structure that contain the imidazole ring as the main component include cimetidine, azomycin, and metronidazole and also have significant application in the various fields [1, 2].

Metal oxide nanoparticles have gained promising research attention due to its exclusive size-dependent optical and electronic properties. They are also applied in various biotechnological fields such as drug delivery, luminescence tagging, and immunoassay. As a result of recent advances in the field, the interaction between organic molecules and the surfaces of the semiconductor materials is an interestingly booming area of research [3 – 6]. An organic molecule on surfaces of the semiconductor leads to the enhanced interaction of the semiconductor with an incident electromagnetic wave [7, 8]. TiO<sub>2</sub> have been applied in the development of various technologies due to their excellent stability, low cost, non-toxicity, and physicochemical property. TiO<sub>2</sub> are generally used to improve their performance in many end-use applications. Reportedly, ethanol suspension of Au/TiO<sub>2</sub>, maintaining charge equilibrium by transferring photoexcited electrons from TiO<sub>2</sub> to Au nanoparticles [5]. Because of the usage of ethanol as a solvent, possible recombination of electrons in Au and holes in TiO<sub>2</sub> has not been studied [11–15]. Various studies have been developed for the quenching of the photoluminescence because of the charge from semiconductor nanoparticles [16–20]. The highest occupied molecular orbital and lowest unoccupied molecular orbital potentials for the designed sensor must match with the conduction and

valence band edges of the semiconductor TiO<sub>2</sub> nanoparticles. In this contribution, we report fluorescence enhancement by TiO<sub>2</sub> nanoparticles by 5-amino-2-mercaptobenzimidazole (fluorochrome). The observed fluorescence enhancement is unique to study the interaction between virgin and Au loaded TiO<sub>2</sub> nanoparticles with fluorochrome.

## 2. Materials And Methods

### 2.1 Reagents

Titanium (IV) isopropoxide was purchased from Sigma Aldrich. Tetrachloro auric acid was obtained from CDH chemicals. Milli-Q- water was used. All other reagents and solvents were used without further purification.

### 2.2 Preparation of Au loaded TiO<sub>2</sub> nanoparticles

Au loaded TiO<sub>2</sub> nanoparticles were prepared by a slight modification of the method described in the literature report [21]. Ti (IV) isopropoxide (20 mM) and acetylacetone (20 mM) in isopropanol (30 ml) was sonicated for 15 minutes. The sonicated solution was added to HAuCl<sub>4</sub>.3H<sub>2</sub>O (10 mM) mixed with milli-Q water (5 ml) and Dimethyl Furan (DMF) (20 ml) was added to it and stirred for 20 minutes. The mixture was then refluxed at 70 °C for 2 h and the precipitate formed was sonicated for 2 h. To this mixture was added toluene and the colloidal material was precipitated, washed with toluene (3 × 10 ml), redissolved in isopropanol. The precipitate was kept at room temperature for 24 h to evaporate the solvent and finally, the Au loaded TiO<sub>2</sub> nanoparticles were isolated.

### 2.3 Instrumentation

XRD diffraction analysis was carried out using X'pert PRO PANalytical diffractometer operated at  $CuK_{\alpha}$  radiation ( $k = 1.5406 \text{ \AA}$ ) source. JEOL JEM-3010 electron microscope was used to take TEM images with the magnification of 600 and 800 k times operated at 300 keV. UV-visible analysis was obtained on Perkin Elmer Lambda 35 spectrophotometer. RXI spectrometer was used to obtain the FT-IR in the frequency range of  $4000-500 \text{ cm}^{-1}$  using the KBr pellets.

### 2.4 Theoretical calculations

The classical point charge model was used to determine the molecular electrostatic potential (MEP). MEP of the molecule has been analyzed by moving a unit positive point charge across the van der Waals surface and calculated at various points ( $j$ ) on this surface using the relation as follows:

$$V_j = q_i / r_{ji}$$

Where,  $q_i$  - partial charge of each atom

$i$  and  $r_{ji}$  - distance between the points  $j$  and atom  $i$

## 3. Result And Discussion

### 3.1 XRD analysis

Figures 1a & b shows the X-ray diffraction patterns of pre and post annealed Au loaded TiO<sub>2</sub> nanoparticles (at 650 °C in air for 5 h). Figure 1a shows three characteristic peaks observed at 37.85, 44.05, and 64.85° (2θ) which originated from (111), (200), and (220) planes of Au respectively (JCPDS No. 89–3697). This shows the face-centered cubic (FCC) structure of Au. The XRD pattern of the air-dried Au loaded TiO<sub>2</sub> has no peak corresponding to TiO<sub>2</sub> nanoparticles, suggesting that the TiO<sub>2</sub> was amorphous. Figure 1b shows the peak at 2θ = 27.35° (101) corresponds to the anatase form of TiO<sub>2</sub>. The average crystal grain size calculated using the Scherrer equation was found to be 46 nm. The patterns are comparable to those reported in the literature [21].

### 3.2 HR-TEM analysis

The HR-TEM images of Au loaded TiO<sub>2</sub> nanoparticles are shown in Figs. 2a & b. Figure 2a shows a collection of core-shell particles. It shows that the particles are evenly distributed. The HR-TEM image of a single Au loaded TiO<sub>2</sub> nanoparticles are shown in Fig. 2b. A closer look at the particles reveals that TiO<sub>2</sub> nanoparticles have been encapsulated with gold. The average particle size is nearly 48 nm. EDX spectrum (Fig. 3) shows that the successful loading of TiO<sub>2</sub> nanoparticles with Au.

### 3.3 Absorption characteristics of fluorochrome - Au loaded TiO<sub>2</sub> nanoparticles

The absorption spectra of the fluorochrome with and without loading of gold and unloaded TiO<sub>2</sub> nanoparticles are displayed in Fig. 4. The fluorochrome absorbance was enhanced by the TiO<sub>2</sub> nanoparticles without the significant changes in the absorption maximum which indicates that nanoparticles do not alter the fluorochrome excitation. The enhancement of absorbance is because of the adsorption of fluorochrome on the TiO<sub>2</sub> surface. The enhanced absorbance by TiO<sub>2</sub> nanoparticles is suppressed by loading it with gold.

### 3.4. Switch on-Switch off fluorescence

Figure 5 shows the emission spectra of fluorochrome in the presence of gold loaded and unloaded TiO<sub>2</sub> nanoparticles. TiO<sub>2</sub> nanoparticles increase the emission of fluorochrome without a change in its emission value which indicates that TiO<sub>2</sub> nanoparticle does not alter the process of excitation. The increased fluorescence inferred with the dispersed TiO<sub>2</sub> nanoparticles as a result of adsorption of the fluorochrome on the surface of TiO<sub>2</sub> semiconductor nanoparticles. The active electron transfer from the excited state of the fluorochrome to the conduction band of the TiO<sub>2</sub> nanoparticle which leads to the increase of fluorescence emission. Fluorescence enhancement arises due to the formation of the complex (fluorophore - nanoparticulate TiO<sub>2</sub>). Loading of TiO<sub>2</sub> by gold shows the dopant inhibits the switch-on

fluorescence by TiO<sub>2</sub> nanoparticles. This is due to the attachment of fluorochrome more strongly to the unloaded TiO<sub>2</sub> nanoparticles than gold loaded TiO<sub>2</sub> nanoparticles.

### 3.5. FT-IR spectral studies

The nature of the interaction between the organic molecule and the semiconductor nanoparticles was further proved by the FT-IR technique. The FT-IR spectra of fluorochrome, fluorochrome functionalized TiO<sub>2</sub> nanoparticle, are displayed in Fig. 6. The band at 1615 cm<sup>-1</sup> assigned to  $\nu(-C=N)$  stretching vibration and the bands at 1526, 1493, and 1467 cm<sup>-1</sup> represents  $-C=C$  aromatic stretching vibration of the fluorochrome. The  $-S-C$  stretching vibration of the mercapto group observed at 1370–1400 cm<sup>-1</sup>. The band observed at 1274 and 1223 cm<sup>-1</sup> corresponds to the  $\nu(C-O)$  stretching vibration of fluorochrome and functionalized TiO<sub>2</sub> nanoparticles, which indicates the bonding is not through phenolic oxygen. The doublet at 1197–1170 cm<sup>-1</sup> and 1132 – 1117 cm<sup>-1</sup> in fluorochrome and functionalized Au loaded TiO<sub>2</sub> nanoparticles assigned to the O = S = O group. The band occurs at 1040 cm<sup>-1</sup> assigned to  $-OCH_3$  group of the fluorochrome. The  $-C-S-H$  stretching vibration of the mercapto group of fluorochrome occurs at 600–632 and 680–756 cm<sup>-1</sup>. The band at 1615 cm<sup>-1</sup> represents the C = N function of the fluorochrome. The slight shift in the fluorochrome modified TiO<sub>2</sub> nanoparticle clearly indicates the binding of TiO<sub>2</sub> nanoparticles on azomethine nitrogen of fluorochrome.

### 3.6. Evidence for linkage

Figure 7 shows the MEP map of fluorochrome contains four basic sites, but in the binding process azomethine ( $>C=N-$ ) nitrogen was involved due to the high electron density. Azomethine nitrogen having higher electron density which has been further proved by density functional theory (DFT) calculation which was used to obtain the MEP for the composites. The dark red region present in the molecular electrostatic potential map represents the most negative potential of the nitrogen atom. The green region predominance in the map represents the potential halfway (red and blue colour) between the two extremes [22].

## 4. Conclusion

A sensitive fluorochrome fluorescent sensor is adsorbed on the surface of Au loaded TiO<sub>2</sub> nanoparticles through active azomethine nitrogen. The position of conduction band energy determines the electron transfer from excited state fluorochrome to Au loaded TiO<sub>2</sub> nanoparticles. The fluorescent enhancement was demonstrated using a photo-induced electron transfer (PET) mechanism. Loading TiO<sub>2</sub> with Au hamper the sensitivity significantly reduces the same. The shift in absorption spectra was observed at 335 nm due to the adsorption of fluorochrome on Au loaded TiO<sub>2</sub> nanoparticles surface. FT-IR results indicate the shift in  $>C=N-$  frequency at 1615 cm<sup>-1</sup> because of the binding of fluorochrome on Au loaded TiO<sub>2</sub> nanoparticles. Azomethine nitrogen plays a major role in the binding process of the fluorescent sensor with Au loaded TiO<sub>2</sub> nanoparticles which were confirmed by MEP studies.

## Declarations

## Competing interest:

No

## References

1. Maojiang Song, Fei Yang, Liping Liu, Caixia Su, Research on differences between 2-(2'-pyridyl)benzimidazole and 2-(4'-pyridyl)benzimidazole based on terahertz time-domain spectroscopy, *Spectrochimica Acta Part A: Molecular and Biomolecular Spectroscopy*, 191 2018, 125-133.
2. Azizollah Nezhadali, Leili Mehri, Raham Shadmehri, Determination of benzimidazole in biological model samples using electropolymerized-molecularly imprinted polypyrrole modified pencil graphite sensor, *Sensors and Actuators B: Chemical*, 171–172, 2012, 1125-1131.
3. Bruchez M, Moronne M, Gin P, Weiss S, Alivisatos A.P, (1998), Semiconductor Nanocrystals as Fluorescent Biological Labels, *Science* 281, 2013-2016.
4. Wu X, Liu H, Liu J, Haley K, Treadway J, Larson J, Ge N, Peals F, Bruchez M, (2002), [Immunofluorescent labeling of cancer marker Her2 and other cellular targets with semiconductor quantum dots](#), *Nat. Biotechnol.* 21, 41-46.
5. Gao X, Cui Y, Levenson R.M, Chung L, Nie S, (2004), In vivo cancer targeting and imaging with semiconductor quantum dots, *Nat. Biotechnol.* 22, 969-976.
6. Choi, H.; Chen, W. T.; Kamat, P. V. Know Thy Nano Neighbor. Plasmonic Versus Electron Charging Effects of Metal Nanoparticles in Dye-Sensitized Solar Cells. *ACS Nano* 2012, 6, 4418–4427.
7. Subramanian, V.; Wolf, E. E.; Kamat, P. V. Catalysis with TiO<sub>2</sub>/Gold Nanocomposites. Effect of Metal Particle Size on the Fermi Level Equilibration. *J. Am. Chem. Soc.* 2004, 126, 4943–4950.
8. Linic, S.; Christopher, P.; Ingram, D. B. Plasmonic-Metal Nanostructures for Efficient Conversion of Solar to Chemical Energy. *Nat. Mater.* 2011, 10, 911–921.
9. Sakshi Bhardwaj, Bonamali Pal, Solar light driven photocatalytic oxidative degradation of methyl viologen using Mn<sup>2+</sup>/Mn<sup>7+</sup>-TiO<sub>2</sub> nanocomposites, *Journal of Photochemistry and Photobiology A: Chemistry*, 393, 2020, Article 112430.
10. Zhaolin Liu, Bing Guo, Liang Hong, Huixin Jiang, Physicochemical and photocatalytic characterizations of TiO<sub>2</sub>/Pt nanocomposites, *Journal of Photochemistry and Photobiology A: Chemistry*, 172, 2005, 81-88.
11. S. Suresh, K. Jayamoorthy, P. Saravanan, S. Karthikeyan, Switch-Off fluorescence of 5-amino-2-mercapto benzimidazole with Ag<sub>3</sub>O<sub>4</sub> nanoparticles: Experimental and theoretical investigations, *Sensors and Actuators B: Chemical* 225, 2016, 463-468.
12. C. Karunakaran, J. Jayabharathi, K. Jayamoorthy, Photoinduced electron transfer from benzimidazole to nano WO<sub>3</sub>, CuO and Fe<sub>2</sub>O<sub>3</sub>. A new approach on LUMO - CB energy-binding efficiency relationship, *Sensors and Actuators B. Chem.*, 182 [2013] 514-520.

13. P. Saravanan, K. Jayamoorthy, S.A. Kumar, [Switch-On fluorescence and photo-induced electron transfer of 3-aminopropyl triethoxysilane to ZnO: Dual applications in sensors and antibacterial activity](#), *Sensors and Actuators B: Chemical* 221 (2015) 784-791.
14. C. Karunakaran, J. Jayabharathi, K. Jayamoorthy, P. Vinayagamoorthy, Inhibition of fluorescence enhancement of fluorochrome on doping ZnO with Cu and Ag, *J. Photochem. Photobiol. A*: 247 [2012] 16-23.
15. S Suresh, K Jayamoorthy, S Karthikeyan, Switch-on fluorescence of 5-amino-2-mercapto benzimidazole by Mn<sub>3</sub>O<sub>4</sub> nanoparticles: Experimental and theoretical approach, *Journal of Luminescence* 198, 2018, 28-33.
16. S. Suresh, S. Karthikeyan, K. Jayamoorthy, [Fluorescence sensing of potential NLO material by bunsenite NiO nanoflakes: Room temperature magnetic studies](#), *Sensors and Actuators B: Chemical* 232, 2016, 269-275.
17. P. Saravanan, K. Jayamoorthy, S.A. Kumar, [Fluorescence quenching of APTES by Fe<sub>2</sub>O<sub>3</sub> nanoparticles–Sensor and antibacterial applications](#), *Journal of Luminescence* 178, 2016, 241-248.
18. J. Jayabharathi, V. Thanikachalam, V. Kalaiarasi, K. Jayamoorthy, Enhancing photoluminescent behavior of 2-(naphthalen-1-yl)-1,4,5-triphenyl-1H-imidazole by ZnO and Bi<sub>2</sub>O<sub>3</sub>, *Spectrochim. Acta Part A* 118 (2014) 182-186.
19. J. Jayabharathi, V. Thanikachalam, V. Kalaiarasi, K. Jayamoorthy, [Characterization and electronic spectral studies of 2-\(naphthalen-1-yl\)-4,5-diphenyl-1H-imidazole bound Fe<sub>2</sub>O<sub>3</sub> nanoparticles](#), *Spectrochim. Acta Part A* 120 (2014) 84-87.
20. C. Karunakaran, J. Jayabharathi, K. Jayamoorthy, P. Vinayagamoorthy, Photoinduced Electron-transfer from benzimidazole to Nanocrystals, *Journal of Molecular Liquids*, 177 (2013) 295-300.
21. T. Renjis. Tom et.al., Freely dispersible Au@TiO<sub>2</sub>, Au@ZrO<sub>2</sub>; Ag@TiO<sub>2</sub> and Ag@ZrO<sub>2</sub> core-shell nanoparticles: One-step synthesis, characterization spectroscopy and optical limiting properties, *Langmuir* 19 (2003) 3439-3445.
22. J. Jayabharathi, V. Thanikachalam, K. Jayamoorthy, Computational studies of 1,2-disubstituted benzimidazole derivatives, *Spectrochim. Acta Part A*: 97 (2012) 131-136.

## Figures

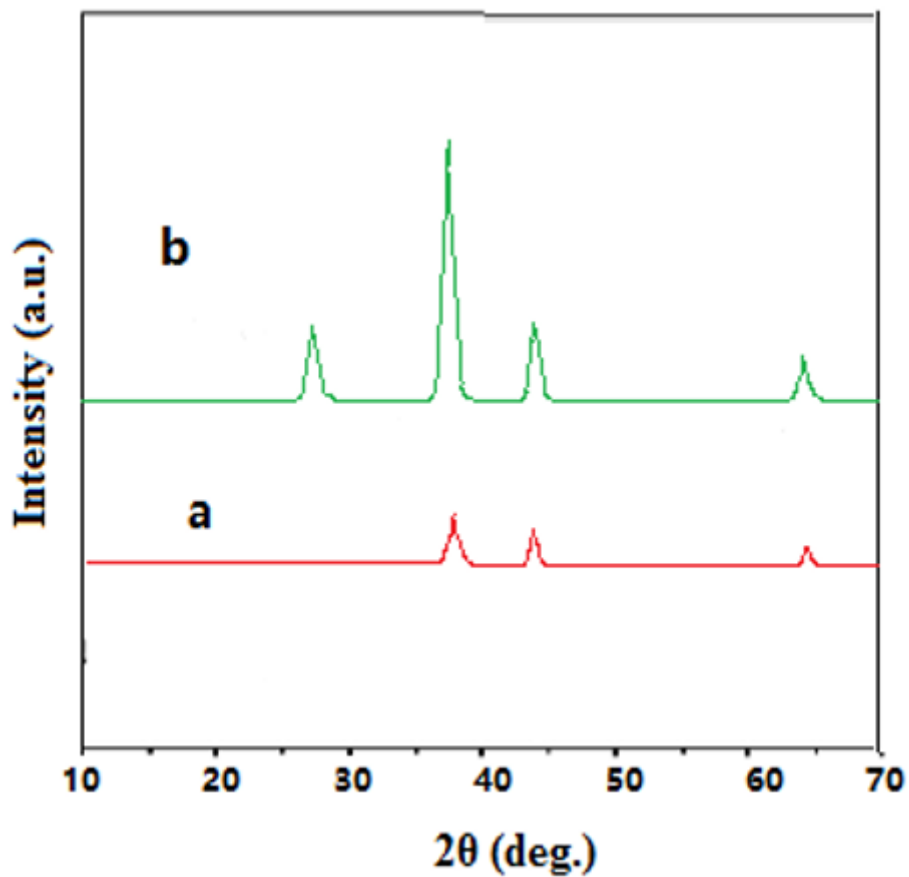


Figure 1

X-Ray diffraction patterns of Au loaded TiO<sub>2</sub> NPs a) air dried sample b) sample annealed at 650 °C

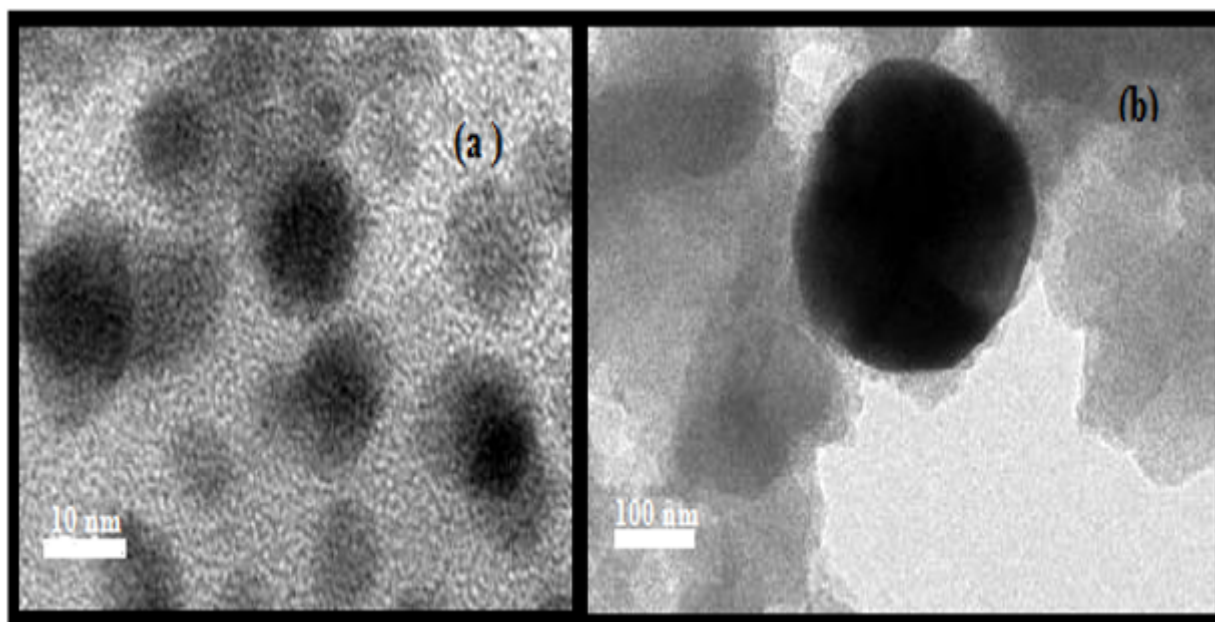


Figure 2

a & b: HRTEM images of Au loaded TiO<sub>2</sub> NPs

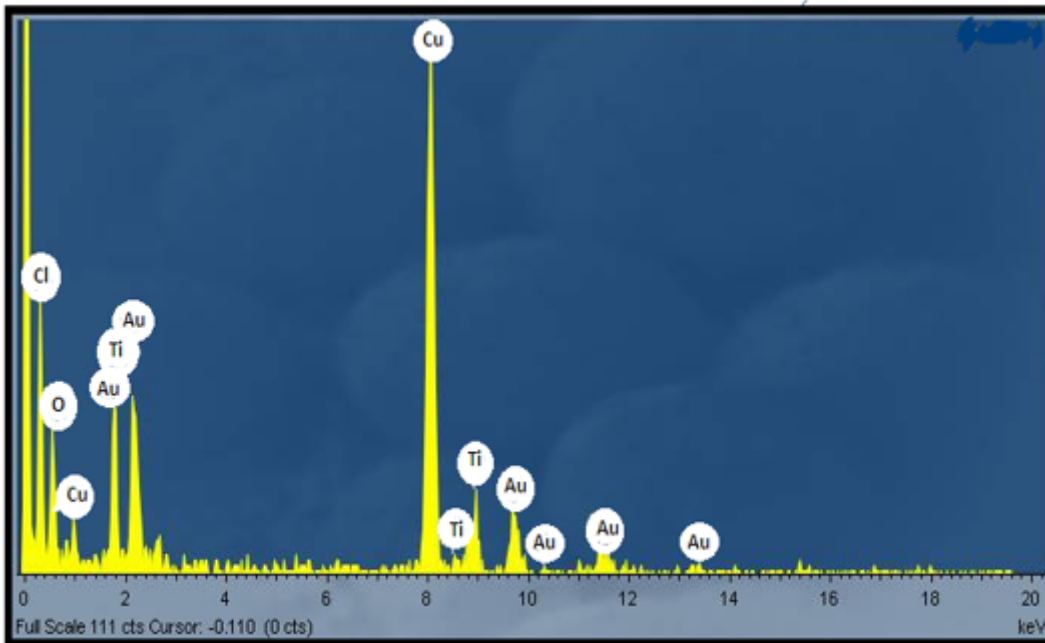


Figure 3

EDX spectrum of Au loaded TiO<sub>2</sub> NPs

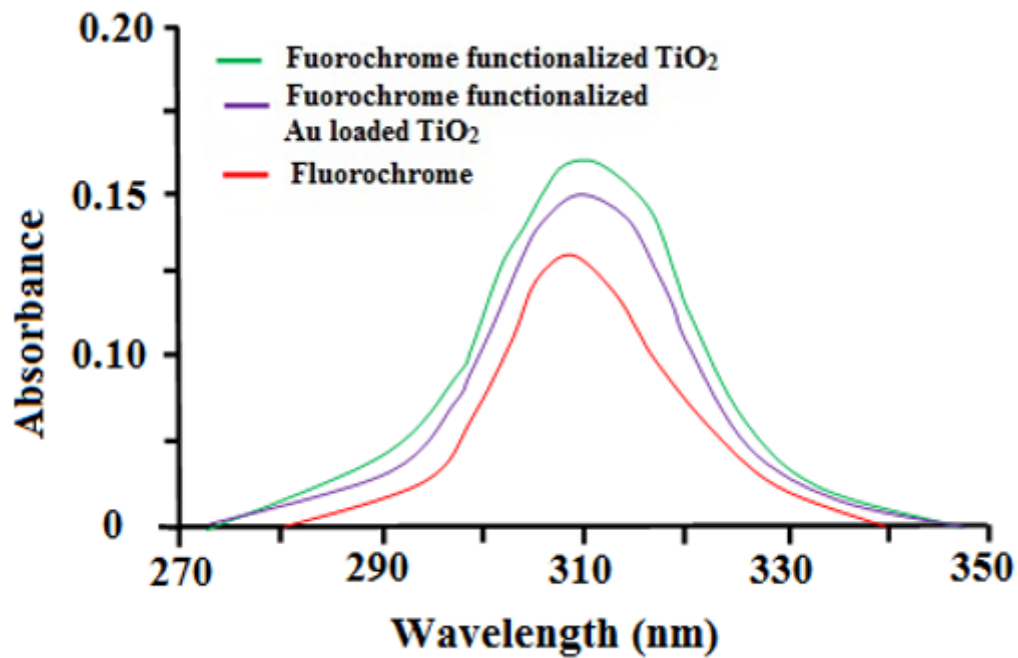


Figure 4

Absorption spectrum of fluorochrome in the presence of gold loaded and unloaded TiO<sub>2</sub> nanoparticles

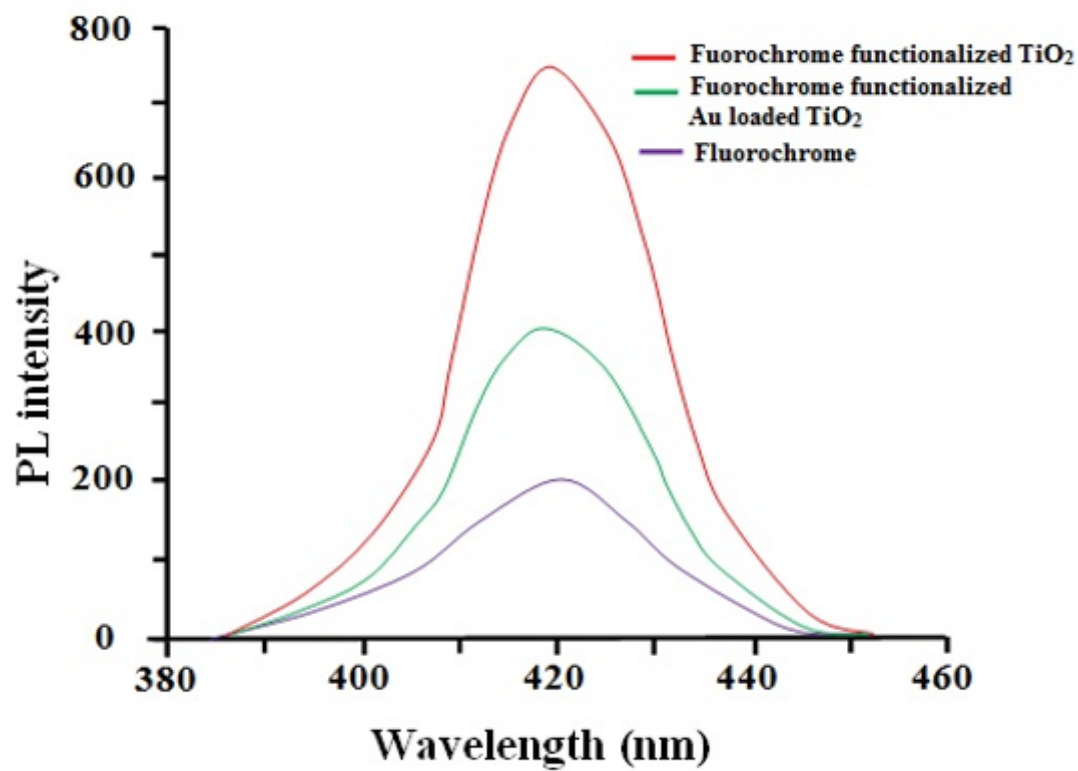


Figure 5

Fluorescence spectrum of fluorochrome in the presence of gold loaded and unloaded TiO<sub>2</sub> nanoparticles

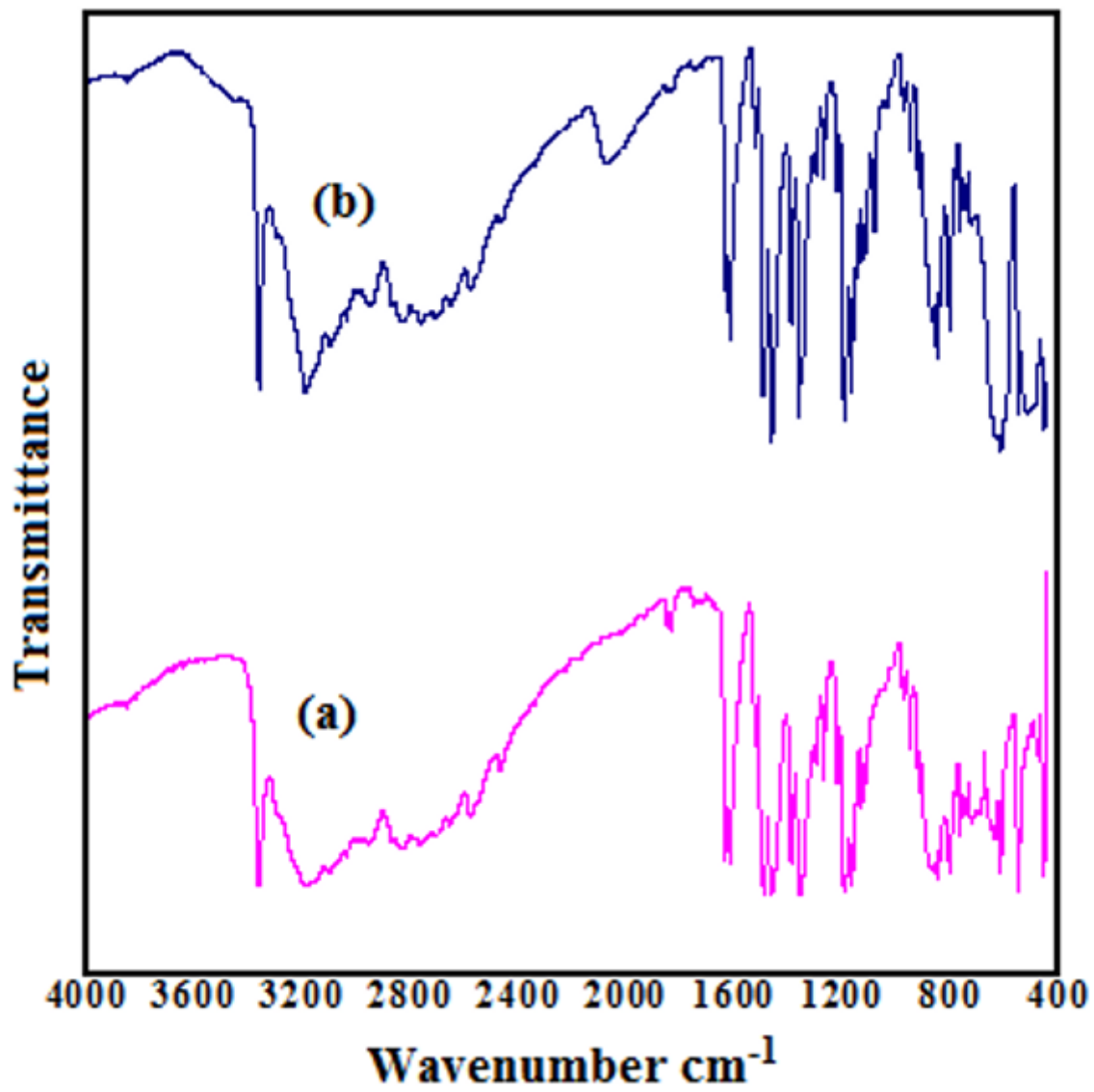


Figure 6

(a) FT-IR spectrum of fluorochrome; (b) fluorochrome functionalized  $\text{TiO}_2$  nanoparticles